ON THE DESIGN OF DIGITAL BROADBAND BEAMFORMER FOR UNIFORM CIRCULAR ARRAY WITH FREQUENCY INVARIANT CHARACTERISTICS

S. C. Chan and Carson K. S. Pun
Department of Electrical and Electronic Engineering
The University of Hong Kong, Pokfulam Road, Hong Kong
scchan@eee.hku.hk,kspun@eee.hku.hk

ABSTRACT

In this paper, the design of digital uniform circular array – frequency invariant beamformer (UCA-FIB) is proposed. After transformation and removal of frequency dependency of the individual phase mode, the frequency invariant phase mode are linear combined with the spatial filter coefficients to form the far field pattern of the array. As the result, such beamformer is a wideband frequency invariant beamformer. For simultaneously beamforming, we propose a UCA-FIB DFT filterbank for concurrent beamforming in different direction. Design examples demonstrated that the proposed UCA-FIB can form deep nulls and sharp peaks with good FI characteristic while the UCA-FIB DFT can spatially divide the array neighboring area into small sectors efficiently.

I. INTRODUCTION

Wideband beamforming using sensor arrays is an effective method for suppressing interference whose angles of arrival are different from the desired looking direction. They find important applications in radio communications, sonar, radar, and acoustics [1-3]. Traditional adaptive wideband beamformer usually employs tapped-delay line with adaptive coefficients to generate appropriate beam patterns for interference suppression. This usually requires considerable number of adaptive coefficients resulting in rather long convergence time and high implementation complexity. This can be remedied by using subband decomposition technique, partial adaptation or the use frequency invariant beamformers (FIB) [4-6,7,9]. In FIB, a beam-forming network is used to generate beam pattern with approximately frequency invariant (FI) characteristic over the frequency band of interest. They can attenuate broadband directional interference using an adaptive beamformer with very few number of adaptive filter coefficients [5].

One of the widely studied FIB is the uniform linear array (ULA) FIB [4-8]. The ULA has a linear geometry with equal inter-sensor spacing. Due to this geometry, its angular resolution at boresight is better than that at its end-fire. In addition, this simple array structure allows many efficient direction of arrival (DOA) detection algorithms. For example, the MUSIC algorithm [10] provides a high resolution method for detecting the angle of arrival (AoA) of the signal sources based on the subspace approach. The MUSIC algorithm can also detect wideband source in beamspace by performing MUSIC in beamspace using ULA-FIB [9]. Besides AoA estimation of wideband sources, adaptive interference suppression using beamspace adaptive beamforming [5] is very attractive because of the small number of adaptive weights required and the possibility of employing partial adaptation, yielding faster convergence and fewer number of high speed variable multipliers.

Given the advantages of ULA-FIB, it is desirable to develop uniform-circular array (UCA) [1] with frequency invariant characteristics. The sensors in a UCA are placed on a circle with uniform inter-sensor spacing. The UCA differs from ULA in the following i) the azimuthal coverage of a UCA is 360^0 in to contrast to 180^0 of that in ULA, ii) the beampattern of UCA is relatively uniform around the azimuth angle while that of ULA broadens as its beam is steered away from the boresight. As for DOA estimation, UCA is suitable for 2D DOA estimation (azimuth and elevation angle) while the ULA is more suitable for azimuth angle DOA estimation [11]. Another interesting property of UCA is that they able to form beam patterns that are relatively invariant with frequency [12].

In this paper, the design of a digital frequency invariant beamformer (FIB) for UCA is proposed. The basic idea is to transform each snapshot sampled by the UCA to the phase modes via an Inverse Discrete Fourier Transform (IDFT). These transformed data is then filtered to compensate for the frequency dependence of the phase modes. Finally, these frequency invariant phase-modes are linear combined using a set of weights or coefficients to obtain the desired frequency invariant beam patterns. These weights, which govern the far field pattern of the UCA, can be designed by conventional 1D digital filter design techniques such as the Parks McClellan algorithm. Alternatively, different beam patterns can be created by varying these coefficients in an adaptive beamformer with approximately frequency invariant characteristics. Using this intrinsic property of UCA, a DFT-based beamspace array can be constructed by modulating a prototype FIB using the DFT basis functions.

The UCA-FIB proposed in this paper find potential applications in acoustic as well as communications. Several design examples are given. Design and simulation results show that the beam patterns of the UCA-FIB are approximately invariant with frequency. In addition, the broadband deep nulls in the adaptive array are very effective in suppressing broadband interference. The paper is organized as follows: In section II, UCA is introduced. In section III, novel digital broadband UCA FIB designed is presented. In section IV, a design example is given. In section V, conclusions are drawn.

II. UNIFORM CIRCULAR ARRAY (UCA)

Figure 1 shows a UCA with K omnidirectional sensors located at $\{r\cos\phi_k, r\sin\phi_k\}$ (represented as Cartesian Coordinate with the center as the origin) where $\phi_k = 2\pi k/K$ and $k = 0,\cdots,K-1$. In UCA, the inter-sensor spacing is fixed at $\lambda/2$ where λ is the smallest wavelength of the array to be operated and is denoted by λ_s. The radius of the UCA is given by

$$r = \lambda_s/(4\sin(\pi/K)), \quad \ldots(1)$$

For convenience, this radius is represented as its normalized version,

$$\hat{r} = r/\lambda_s = 1/(4\sin(\pi/K)) \quad \ldots(1a)$$

The phase difference between the k^{th} sensor and the center of the UCA is $\chi_k = \pi r\sin\theta\cos(\phi-\phi_k)/\lambda$, and the corresponding phase shift is $e^{j\omega\hat{r}\sin\theta\cos(\phi-\phi_k)}$, where ϕ, and θ are the azimuth angle and the elevation angle respectively, as shown in figure 3. Hence, the steering vector [1] of a UCA is

0-7803-7448-7/02/$17.00 ©2002 IEEE

$$s=\left[e^{j\omega\hat{r}\sin\theta\cos(\phi-\phi_0)} \quad e^{j\omega\hat{r}\sin\theta\cos(\phi-\phi_1)} \quad \cdots \quad e^{j\omega\hat{r}\sin\theta\cos(\phi-\phi_{K-1})}\right] \quad \ldots(2)$$

The azimuth angle ϕ is on the horizontal plane where the sensors are situated. It measures from a reference imaginary axis on this horizontal plane, while the elevation angle θ is measured from a reference imaginary axis perpendicular to the horizontal plane. Without loss of generality, our design will be focused at an elevation angle of $\theta=\pi/2$, i.e. the horizontal plane.

III. DIGITAL BROADBAND UCA FIB

Figure 4 shows the structure of the broadband FIB for the UCA. After appropriate downconverting, lowpass filtering and sampling, the sampled signal after the antenna is given by the vector $X[n]=[x_0(n) \quad x_1(n) \quad \cdots \quad x_{K-1}(n)]^T$ which is called a snapshot at sampling instance n. This snapshot is IDFT transformed to the phase-mode and the transformed snapshot is denoted by $V[n]=W_{MK}\cdot X[n]$, where W_{MK} is an M by K IDFT matrix with $\left[W_{MK}\right]_{m,k}=e^{j2\pi mk/K}$ and

$$[V[n]]_m=v_m[n]=\sum_{k=0}^{K-1}x_k[n]e^{j\frac{2\pi km}{K}} \quad \ldots(3)$$

We assume that M is an odd number. Each branch of the IDFT output is then filtered by $H_m(\omega)$ (to compensate for the frequency dependency as we shall see later in this section), multiplied with g_m before combining to give the beamformer output $y[n]$:

$$y[n]=\sum_{m=0}^{M-1}\left(v_m[n]*h_m[n]\right)\cdot g_m, \quad \ldots(4)$$

where * denotes discrete-time convolution. To obtain the spatial-temporal transfer function of the beamformer, let's assume that there is only one source signal $s(n)$ with spectrum $S(\omega)$. Taking the Discrete Time Fourier Transform (DTFT) of equation (3), one gets

$$V_m(\omega)=\sum_{k=0}^{K-1}X_k(\omega)e^{j\frac{2\pi km}{K}}=S(\omega)\sum_{k=0}^{K-1}e^{j\omega\hat{r}\cos(\phi-\phi_k)}e^{j\frac{2\pi km}{K}}. \quad (5a)$$

Taking DTFT on both size of equation (4) and using eqn. (5a), we have

$$\begin{aligned}Y(\omega)&=\sum_{m=-M/2}^{M/2}g_mV_m(\omega)H_m(\omega)\\&=\sum_{m=-M/2}^{M/2}g_m\sum_{k=0}^{K-1}X_k(\omega)e^{j\frac{2\pi km}{M}}H_m(\omega) \quad \ldots(5b)\\&=S(\omega)\sum_{m=-M/2}^{M/2}g_m\left(\sum_{k=0}^{K-1}e^{j\omega\hat{r}\cos(\phi-\phi_k)}e^{j\frac{2\pi km}{K}}\right)H_m(\omega)\end{aligned}$$

Hence, the spatial-temporal response of the beamformer is

$$G(\omega,\phi)=\sum_{m=-M/2}^{M/2}g_m\left[\sum_{k=0}^{K-1}e^{j\omega\hat{r}\cos(\phi-\phi_k)}e^{j\frac{2\pi km}{K}}H_m(\omega)\right] \quad \ldots(6)$$

To obtain a frequency invariant response, it is desirable to have the term inside the bracket be independent on frequency variable ω. First of all, using the expansion [13],

$$e^{j\alpha\cos\gamma}=\sum_{n=-\infty}^{+\infty}j^nJ_n(\alpha)e^{jn\gamma}, \quad \ldots(7)$$

where $J_n(\alpha)$ is the Bessel function of the first kind, (6) can be rewritten as

$$\begin{aligned}G(\omega,\phi)&=\sum_{m=-M/2}^{M/2}g_m\sum_{k=0}^{K-1}\sum_{n=-\infty}^{+\infty}j^nJ_n(\omega\hat{r})e^{jn(\phi-2\pi k/K)}e^{j\frac{2\pi km}{K}}H_m(\omega)\\&=\sum_{m=-M/2}^{M/2}g_mH_m(\omega)\sum_{n=-\infty}^{+\infty}j^nJ_n(\omega\hat{r})e^{jn\phi}\left(\sum_{k=0}^{K-1}e^{j2\pi k\left(\frac{m-n}{K}\right)}\right)\end{aligned} \quad (8)$$

Further, the term inside the bracket is evaluated to be

$$\sum_{k=0}^{K-1}e^{j2\pi k\left(\frac{m-n}{K}\right)}=\begin{cases}K & m-n=Kp\\0 & otherwise\end{cases}, \quad where \quad p\in Z. \quad \ldots(9)$$

Substituting (9) into (8) gives

$$G(\omega,\phi)=K\sum_{m=-M/2}^{M/2}g_m\left[\sum_{n=m+Kp}j^nJ_n(\omega\hat{r})e^{jn\phi}\right]H_m(\omega) \quad \ldots(10)$$

From [13], the Bessel function has the following property

$$\left|J_{|n|}(\omega\hat{r})\right|\le\left(\frac{\omega\hat{r}e}{2|n|}\right)^{|n|}. \quad \ldots(11)$$

Therefore, for sufficiently large value of n, the value of the Bessel function will be negligibly small. In other words, if the number of sensors is large enough (say n>8), $G(\omega,\phi)$ can be approximated by

$$G(\omega,\phi)\approx K\sum_{m=-M/2}^{M/2}g_m\left[j^mJ_m(\omega\hat{r})H_m(\omega)\right]\cdot e^{jm\phi} \quad \ldots(12)$$

If we design the filters $H_m(\omega)$ to compensate for the frequency dependency in each mode m, that is

$$H_m(\omega)\approx j^{-|m|}/(KJ_{|m|}(\omega\hat{r})) \text{ for } \omega\in[\omega_L,\omega_U], \quad \ldots(13)$$

where ω_L and ω_U are respectively the lower and upper frequencies of interest, then the beamformer in (12) will be approximately frequency invariant within $\omega\in[\omega_L,\omega_U]$ and

$$G(\phi)\approx\sum_{m=-M/2}^{M/2}g_me^{jm\phi}. \quad \ldots(14)$$

Furthermore, its far field pattern is now governed by the spatial weighting $\{g_m\}$ alone. From equation (14), it can be seen that the far field spatial response is similar to that of a digital FIR filter with impulse response $\{g_m\}$. Therefore, $G(\phi)$ can be designed by conventional filter design algorithms such as the Parks-McClellan algorithm. In addition, angular shifted versions of equation (14) can be derived by modulating $\{g_m\}$ with sinusoids at appropriate frequencies. For example, if the shift is $\pi/2$, then the modulation is $\{e^{j\frac{\pi}{2}m}\}$, $m=-M/2,\ldots,M/2$. Further, a broadband beamspace array with equally spaced angles can readily and efficiently be implemented using the basis functions of the DFT. Real-time adaptation of the beam pattern to suppress undesired interference is also simpler than traditional broadband adaptive array using tapped delay lines. We now consider some design examples.

IV. DESIGN EXAMPLES

Example 1: Broadband narrow beamwidth UCA-FIB.

In this example, a 16-element UCA with omnidirectional sensors is considered. The required bandwidth of the UCA-FIB is $\omega\in[0.3\pi,0.75\pi]$. The number of phase modes M is 11. Therefore we have 11 spatial filter coefficients to shape the spatial response of the UCA FIB. The desired beam is targeted at 60^o and the beamwidth is 5^o. $\{g_m\}$ are obtained from the Parks-McClellan algorithm according to the given specification with same passband and stopband ripples. The frequency responses are shown in figures 5 and 6. In figure 5, for convenience, the frequency responses of the UCA-FIB for $\omega\in[0.3\pi,0.75\pi]$ are overlapped together to illustrate the frequency invariant property of the beamformer. The frequency spectrum is approximately FI, with deep nulls formed at the desired position over the bandwidth of interest. Figure 6 shows the perspective view of the beamformer.

Example 2: Broadband wide beamwidth UCA-FIB for sectored communications.

In this example, a 12-element UCA will be considered. The required FI bandwidth of the UCA-FIB is $\omega \in [0.3\pi, 0.75\pi]$. The number of phase mode M is 11. Therefore 11 spatial filter coefficients can be used to shape the FIB-UCA spatial response. The desired beam is targeted at -20^o and the beamwidth is 60^o. Again, $\{g_m\}$ is designed using the Parks McClellan algorithm with the given specification and identical passband and stopband ripples. The frequency responses of the FIB in the range $\omega \in [0.3\pi, 0.75\pi]$ is shown in figure 7. Again, the frequency spectrum is approximately FI with deep nulls formed at the desired position.

Example 3: Beamspace DFT filter bank

In this example, the concept of DFT-beamspace FI beamformer will be illustrated. The beamformer in this example has 12 sensors and 11 phase modes. 4 FI beams are going to be designed using our proposed UCA-FIB DFT-beamspace beamformer. The beamwidth is 45^0 and the center spatial frequencies of the beams are located at -155^0, -110^0, -65^0, -20^0, 25^0, 70^0, 115^0, 160^0. (i.e. the consecutive beam spacing is 45^0) All the beams are derived from the same spatial filter by modulating the coefficient of a prototype filter. Since the modulation forms a DFT matrix, the beams in the UCA-FIB-DFT beamspace array can be formed using a single UCA-FIB followed by a DFT. The frequency response is plotted in figure 8 for $\omega \in [0.3\pi, 0.75\pi]$. It can be seen that the UCA-FIB-DFT beamspace array simply divides the spatial response into 8 sectors or subbands, with each beam points at the desired direction. Again, the beampattern is approximately FI and forms deep nulls over the frequency band of interest.

V. Conclusion

The theory and design of digital UCA FIB is presented. After transforming to individual phase mode and removing its frequency dependency using a set of digital filters, the far field pattern is approximately independent of frequency and is defined by the linear combination of a set of spatial filter coefficients. The UCA-FIB spatial characteristic can then be controlled by these spatial filter coefficients, which can be designed easily using conventional one dimensional digital filter design algorithms. A UCA-FIB DFT beamspace array for simultaneously sectoring of the spatial response of the array into subbands is also proposed. Design examples demonstrated that the proposed techniques yield UCA with approximately frequency invariant characteristics capable of yielding deep nulls over a wide bandwidth. The proposed UCA-FIB is expected to find applications in acoustic and wireless communications. Preliminary wideband adaptive beamforming and angle of arrival estimation using the proposed array show very promising results. The details will be reported in future work.

References

[1] D. H. Johnson and D. E. Dudgeon, *Array signal processing: concepts and techniques*, Prentice Hall, 1993.

[2] H. Krim and M. Viberg, "Two decades of array signal processing research: the parametric approach," *IEEE Signal Processing Mag.*, vol. 13, pp. 67-94, Jul. 1996.

[3] B. D. Van Veen and K. M. Buckley, "Beamforming: a versatile approach to spatial filtering," *IEEE ASSP Mag.*, vol. 52, pp. 4-24, Apr. 1988.

[4] K. Nishikawa, T. Yamamoto, K. Oto and T. Kanamori, "Wideband beamforming using fan filter," in *Proc. IEEE ISCAS*, vol. 2., pp. 533-536, 1992.

[5] T. Sekiguchi and Y. Karasawa, "Wideband beamspace adaptive array utilizing FIR Fan filters for multibeam forming," *IEEE Trans. Signal Processing*, vol. 48, pp. 277-284, Jan. 2000.

[6] D. B. Ward, R. A. Kennedy and R. C. Williamson, "Theory and design of broadband sensor arrays with frequency invariant far-field beam patterns," *J. Acoust. Soc. Amer.*, vol. 97, no.2, pp.1023-1034, Feb. 1995.

[7] D. B. Ward, R. A. Kennedy and R. C. Williamson, "FIR filter design for frequency invariant beamformers," *IEEE Signal Processing Lett.*, vol.3, pp. 69-71, Mar. 2000.

[8] M. Ghavami and R. Kohno, "Recursive fan filters for a broad-band partially adaptive antenna," *IEEE Trans. Commun.*, vol. 48, pp.185-188, Feb. 2000.

[9] D. B. Ward, Z. Ding and R. A. Kennedy, "Broadband DOA estimation using frequency invariant beamforming," *IEEE Trans. Signal Processing*, vol. 46, pp. 1463-1469, May 1998.

[10] R. O. Schmidt, "Multiple emitter location and signal parameter estimation," *IEEE Trans. Antennas Propagat.*, vol. AP-34, pp. 276-280, Mar. 1986.

[11] C. P. Mathews and M. D. Zoltowski, "Eigenstructure techniques for 2-D angle estimation with uniform circular arrays," *IEEE Trans. Signal Processing*, vol. 42, pp. 2395-2407, Sep. 1994.

[12] H. Steyskal, "Circular array with frequency-invariant pattern," *Antennas and Propagation Society International Symposium 1989*, AP-S. Digest, vol. 3, pg. 1477-1480, 1989.

[13] M. Abramowitz and I. A. Stegun, *Handbook of Mathematical Functions*, New York: Dover, 1965.

Figures

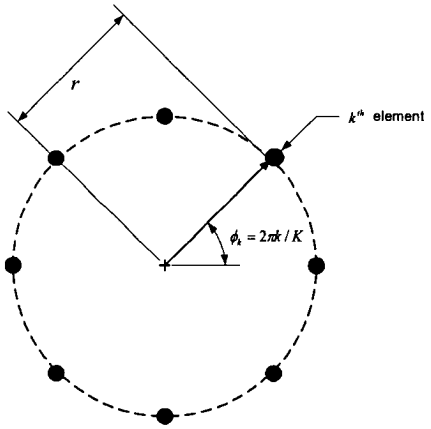

Figure 1. A uniform circular array with K-sensor.

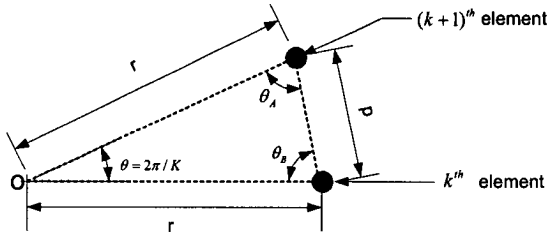

Figure 2. Relationship between inter-sensor spacing and the radius of the UCA.

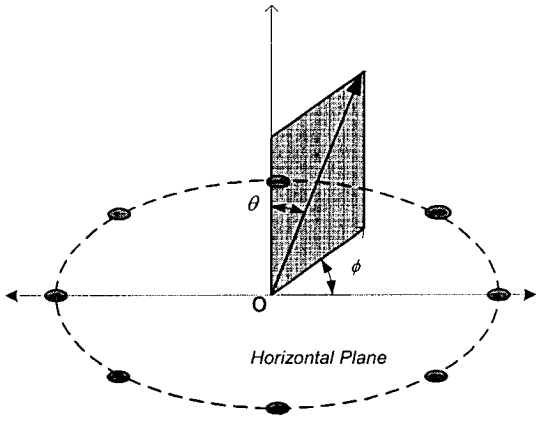

Figure 3. Geometry of the reference imaginary frame.

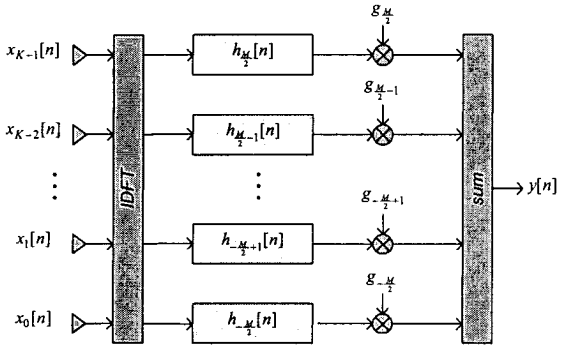

Figure 4. UCA-FIB block diagram.

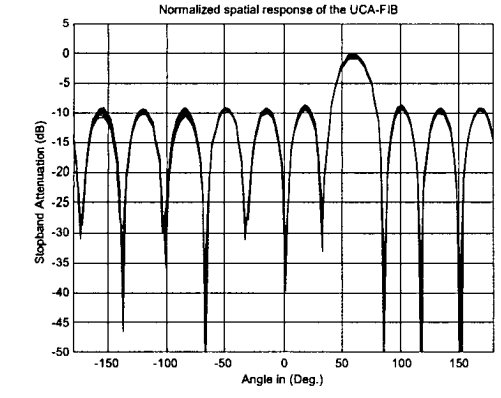

Figure 5. Spatial response of the UCA-FIB with 12 elements and 11 phase modes for $\omega \in [0.3\pi, 0.75\pi]$.

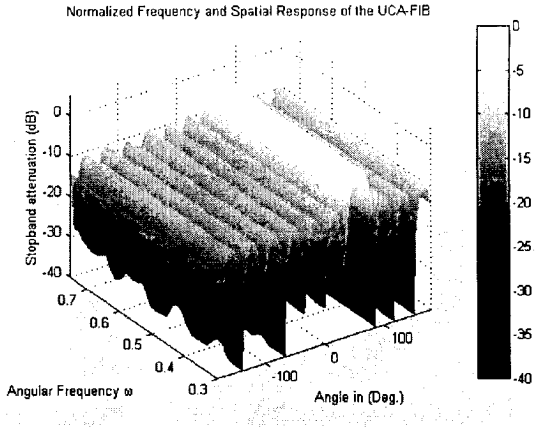

Figure 6. Spatial response and frequency response of the UCA-FIB with 12 elements and 11 phase modes for $\omega \in [0.3\pi, 0.75\pi]$.

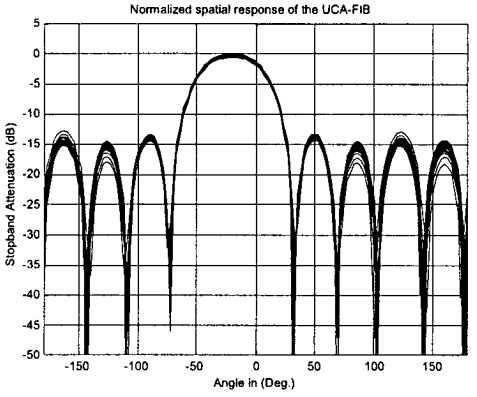

Figure 7. Spatial response of the UCA-FIB with 12 elements and 11 phase modes for $\omega \in [0.3\pi, 0.75\pi]$.

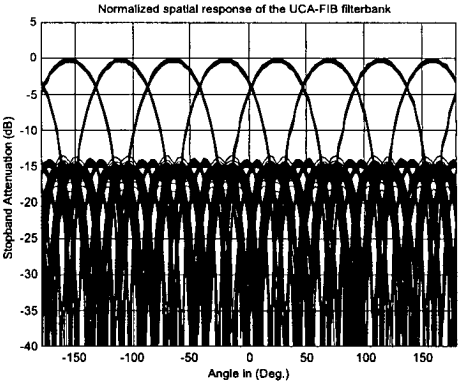

Figure 8. Spatial response of the UCA-FIB DFT filterbank for $\omega \in [0.3\pi, 0.75\pi]$.